Materials Science in Semiconductor Processing 12 (2009) 175–184

Contents lists available at ScienceDirect

Materials Science in Semiconductor Processing

journal homepage: www.elsevier.com/locate/mssp

Study of minority carrier injection phenomenon on Schottky and plasma deposited p–n junction diodes

Orhan Özdemir [a,*], Kıvanç Sel [b]

[a] Yildiz Technical University, Physics Department, Davutpaşa, İstanbul, Turkey
[b] Çanakkale Onsekiz Mart University, Physics Department, Çanakkale, Turkey

ARTICLE INFO

Available online 4 November 2009

Keywords:
Conductivity modulation
Minority carrier injection

ABSTRACT

Both temperature dependent ac capacitance (C) together with ac conductance (G) under various frequencies (ω) and dc current (I) measurements as functions of bias (V) were employed to investigate majority as well as minority carrier injection phenomenon on chromium-p-type crystalline silicon (Cr/p-cryst. Si/ohmic contact) Schottky and aluminum/plasma deposited n-type hydrogenated amorphous silicon/p-c-Si (Al/n-a-Si:H/p-c-Si/ohmic contact) p–n structures. Ambipolar transport process was eventual for both diodes and behaved differently according to the mentioned techniques: for a well defined forward bias interval, there was an increase in capacitance towards maximum that interpreted as majority carrier injection from the back electrode. On the other side, minority carrier injection from front electrode begun when the bias went beyond the critical voltage (i.e., built-in voltage) that corresponded to the peak position and caused sharp decrease in measured capacitance, leading to observation of a hump in C–V measurement. Moreover, shape and peak position of the hump were frequency/temperature dependent. Remarkably, in the bias range where capacitance pronounced, space charge limited current (SCLC) was discerned as enrolled carrier flow mechanism according to I–V measurement, confirming further majority carrier injection. In addition, both dc conductivity and ac conductance followed the same dependence with bias voltage in forward direction. On the other side, reverse current seemed proportional to square root of reverse bias, implying generation current in the depletion region. These experimental identifications convinced us of the existence of conductivity modulation issue for the structures at hand.

1. Introduction

Irrefutably, metal/semiconductor (MS) Schottky and p–n junctions play an essential role in electronic technology and they are also widely used as investigating tools for emerging semiconductors such as organic/inorganic materials [1–4]. These junctions depend on majority carriers where mostly minority carrier injection issue is ignored. However, in some cases, this phenomenon though unappreciated plays a key role where injection of electrons into p-type crystalline silicon (p-c-Si) from the metal electrode could not be negligible anymore at high forward biases and becomes significant in surveying techniques, namely dc current–voltage (I–V) and ac admittance (Y=G+jωC where G=ac conductance and C=capacitance) measurements, respectively. In other words, in Schottky diodes, electrons are injected from the metal side whereas holes are injected from the semiconductor and hence bipolar (ambipolar) transport process occurs [5]. To do so, barrier height ϕ_{Bn} for electrons (minority carriers) should be low and hence

* Corresponding author. Tel.: +90 212 383 4279; fax: +90 212 449 1514.
E-mail address: ytu.orhan@gmail.com (O. Özdemir).

1369-8001/$ - see front matter © 2009 Elsevier Ltd. All rights reserved.
doi:10.1016/j.mssp.2009.10.001

remaining barrier for holes ϕ_{Bp} (majority carriers) must be high since their sum shall be equal to the energy band gap (E_G) of the semiconductor. In this view, for the case of $\phi_{Bp} > E_G/2$, injection is usually unavoidable and produce inversion layer where minority carriers surpass majority ones ($n > p$). Under the appropriate bias application, some of these injected minorities diffuse towards the neutral region of the semiconductor whilst an equal amount of opposite majorities should enter from the back electrode to maintain charge neutrality [6]. Consequently, modulation of conductivity occurs and manifests itself as reducing in diode series resistance (R_s) and hence improves the rectification ratio (forward current/reverse current) in I–V measurement. For the admittance measurement, on the other hand, diffusion of minority carriers have drastic influence on C_m G_m (as in the case of dc conductivity) behavior in the forward bias voltage (accumulating type bias), especially at low frequency. In other words, while bias is scanned under low frequency in the C–V measurement, the capacitance increases until a point where it reaches maxima and decreases sharply afterwards. That is there would be a hump whose shape and peak position depend on bulk resistivity and nature of the metal contacts [3]. Besides, maxima of the hump decrease with increase in both frequency and forward bias voltage. Similar analysis to the one outlined above for Schottky diode could also be carried out for p–n junction by following a different path.

In this work, both junctions were produced to study minority carrier injection issue through I–V in conjunction with $C_m(G_m/\omega)$–V measurements.

2. Sample fabrication and measuring system

Three (1 0 0) oriented boron doped p-type silicon wafers (1–3 Ω cm) were cleaned with standard RCA cleaning procedure. Prior to fabricate Schottky and p–n junctions, rear sides of two of them were coated by aluminum (Al) and then annealed in nitrogen ambient at 530 °C to form ohmic back contacts for electrical analysis. One of them was used for producing Schottky diode where e-beam system was handled to evaporate chromium(Cr) metal on the front face of p-c-Si through a shadow mask. The other one (p-c-Si/ohmic back contact) together with previously chemically cleaned Al coated and corning glass substrates were loaded into the chamber of plasma enhanced chemical vapor deposition (PECVD) system to deposit n-type a-Si:H. Growth of n-type a-Si:H was achieved with the following deposition conditions: RF power was settled to 40 W and phosphine (PH_3) and silane (SiH_4) gases were introduced into the chamber of PECVD reactor with 200 and 20 ccm flow rates, respectively. The pressure of chamber was kept constant at 0.5 Torr during deposition and then the system was stopped after 40 min. Finally, utilizing circular and planar masks, Al was evaporated to complete sandwich and planar configurations as Al/n-a-Si:H/p-c-Si/ohmic back contact and Al/n-a-Si:H/Al coated glass, respectively.

By means of optical transmission measurement through a UV–Visible spectrometer (λ2S, Perkin Elmer), refractive index (n), optical energy gap (E_G) and thickness of the film (d) were obtained via the Swanapole envelope method and a characterization software, OptiChar. Keeping in mind in data analysis that E_G is defined as an energy point in the absorption spectrum where the absorption coefficient reaches $10^4\,cm^{-1}$. Thickness of the film was also measured by XP-2 Ambios thickness profiler that requires a step between film and substrate (i.e., groove). Also, through measurement of IR spectrum (FTIR, Nicolet 520), information on the film structure at hand was obtained.

For electrical analysis, on the other hand, I–V and $C(G/\omega)$–V_G characteristics were reported at room temperature in evacuated cryostat in dark condition by Keithley 6517 multimeter and HP4192A LCR meter, respectively. For the studied temperature interval (200–400 K), helium closed cycle cryostat equipped with temperature controller was used. Experiments were performed through a LABVIEW program.

3. Results

3.1. Optical characterization

Optical transmittance measurements were reported in the range 200–1100 nm on an n-a-Si:H/corning glass substrate. Optical properties of the films such as n, E_G as well as d and their variations along the radial direction (R) of bottom electrode of the PECVD reactor are depicted in Fig. 1a. As R changes from −30 to 120 mm, n (3.6) and E_G (1.9 eV) stayed constant whereas d was doubled after 80 mm. Since Si substrates were placed around 65 mm of bottom electrode in deposition, thickness of the film could also be declared as independent of R and was obtained as 340 nm for both investigated techniques (see Fig. 1a).

The IR spectrum of n-type a-Si:H film deposited on Si substrate consists of two main absorption bonds in the wavenumber ranges 500–1500 and 1900–2200 cm^{-1} (see Fig. 1b). Since each bond represents different vibration modes, they were separately deconvolved and the resultant peaks and their assignments were presented in Table 1.

Apart from optical analysis, resistivity of the film at hand confirmed the amorphous state and is illustrated in Fig. 1c. Log–log plot of I–V measurement on Al/n-a-Si:H/Al coated glass structure had linear dependence at room temperature which indicated (i) metal electrodes were not blocking type and (ii) high bulk resistance of a-Si:H film was observed as predicted [6,18].

3.2. Electrical characterization

As declared before, minority carrier injection onsets under certain value of forward bias voltage and exhibite as a reduction in series resistance of the structure at hand in I–V measurement and observing a hump like behavior in C–V curve. From now on, I–V and C–V behavior of Schottky and p–n junctions would be presented in forward bias direction before and after the mentioned bias voltage range, respectively.

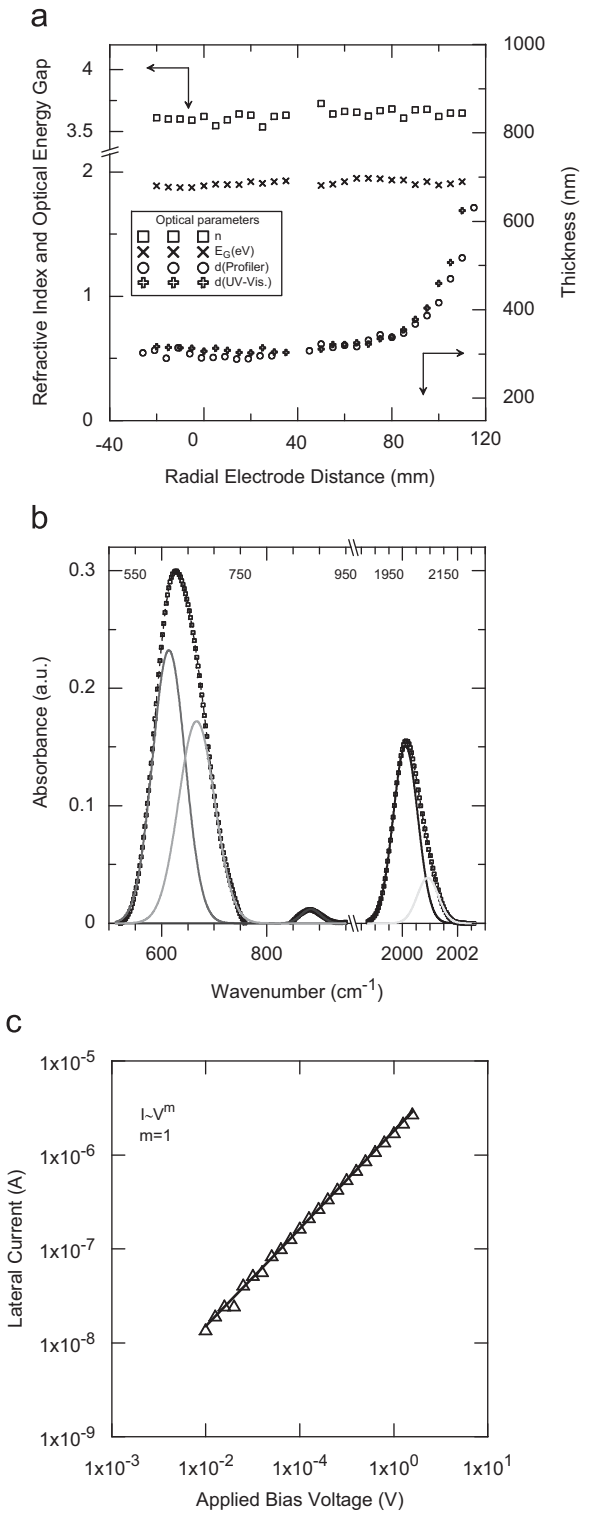

Fig. 1. (a) Refractive index (n), optical energy gap (E_G) and thickness (d, determined by profiler and UV–Vis measurements) variation for n-type a-Si:H thin film with respect to the position of the samples along the radial (R) direction of the bottom electrode of the PECVD reactor. Note that R=0 denotes the center and R=120 mm is the edge of the electrode. (b) Assignments of absorption peaks in FTIR spectrum of a-Si:H thin film. (c) Room temperature I–V measurement of Al/a-Si:H/Al film in lateral configuration.

Table 1
Assignments of absorption peaks in FTIR spectra of a-Si:H thin films.

Peak no.	Wavenumber (cm^{-1})	Bond type and mode of vibration
P1	640	Si–H, wagging [7–9]
P2	670	Si–H_n wagging [10–13]
P3	850–900	$(Si–H_2)_n$ bending [9,14,15]
P4	2000	Si–H, stretching [9,11,13,15–17]
P5	2090	Si–H_2, stretching [10,11,13,15,17]

3.2.1. *I–V behavior of Schottky and p–n junctions*

Figs. 2 and 3 depict temperature dependent I–V characteristics of Schottky (Cr/p-Si/ohmic back contact) and p–n (Al/n-a-Si:H/p-c-Si/ohmic back contact) structures, respectively. It is obvious that junctions have rectifying features for the bias range of 3 kT/q and ~0.2 V where R_s is negligible and hence relationship of I–V behavior should obey the well known diode equation

$$I = I_0 \exp(\beta V - 1)$$

with

$$I_0 = SA^*T^2 \exp(-\beta\phi_{Bp}) \quad \text{and} \quad \beta = \frac{q}{kT}$$

where S=electrode area of diodes, A^*=Richardson constant, q=elementary charge, k=Boltzmann constant, ϕ_{Bp}=barrier height and I_0= saturation constant. This is the ideal Schottky diode I–V expression, based on the thermionic emission model. For non-ideal case, the relation would be modified as

$$I = I_0 \exp\left(\frac{\beta V}{\eta} - 1\right)$$

where η is dimensionless constant, known as ideality factor of diode. Frankly speaking, η and ϕ_{Bp} are the fundamental diode parameters and η would be equal to unity provided the thermionic emission model is the governing carrier flow mechanism. Another mechanism simply causes to deviate η from unity. Moreover, through temperature dependence, dominant current mechanism could be found out. Shortly, A(=β/η) would be temperature independent for tunneling, q/kT for diffusion and q/2kT for recombination models [5–6]. Meanwhile, ϕ_{Bp} parameter turns into activation energy (E_A) and it is equal to energy gap of the semiconductor ($\sim E_G$) for diffusion and E_G/2 for recombination models.

Apart from these aforementioned models, combination of these mechanisms such as multistep tunneling capture emission (MSTCE) [19] and minority carrier injection current models are also possible under forward bias condition [1–4].

Keeping the whole historic information in mind, let us analyse the I–V measurement. As shown in Figs. 2b and 3b, slopes of ln$I$ vs. V plot stay constant for different temperatures (see Table 2) in forward bias direction, implying a tunneling mechanism. On the contrary, I_0 has exponential $-1/T$ dependence rather than T and this is illustrated in Figs. 2c and 3c for the structures at hand. Consequently, combination of tunneling and recombination model, namely MSTCE mechanism, might probable hold for the present system. In other words,

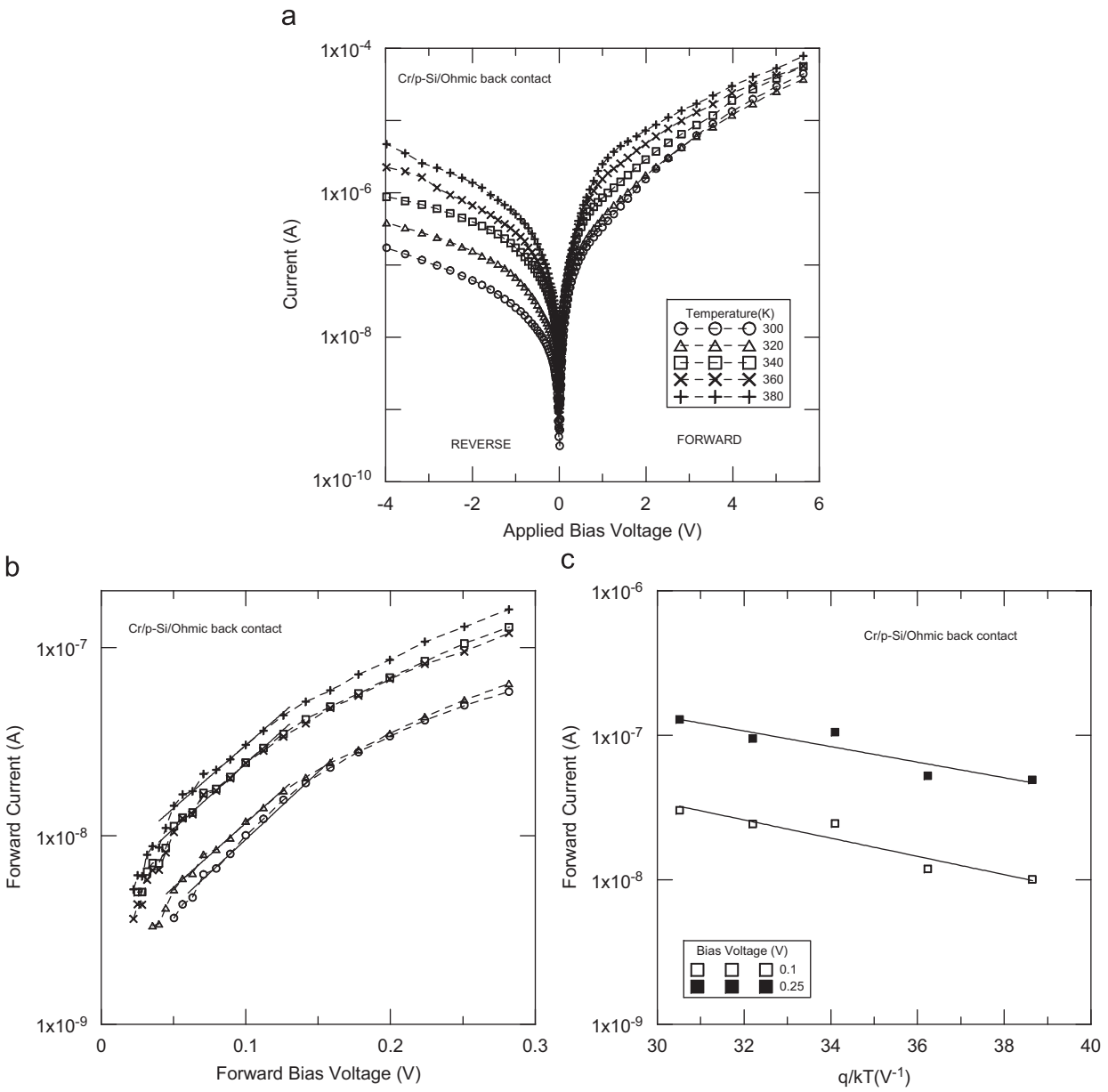

Fig. 2. (a) Forward–reverse *I–V* characteristic of Cr/p-c-Si/ohmic back contact Schottky diode for the studied temperature interval (300–380 K). (b) The $\ln I_F$ vs. V_F variation of Schottky diode. Note that between 3 kT/q and ~0.2 V, temperature independent current mechanism dominates the current flow in the studied temperature interval. (c) Temperature dependence of forward current of Schottky diode at two different forward bias voltages.

holes injected from the ohmic back contact of p-c-Si flows by tunneling within the depletion region of n-a-Si:H until recombining with the electron which supplied from conduction band of a-Si:H. Hence, the current equation for p–n diode would be

$$I_{pn} = I_{0,\,pn} \exp(AV)$$

with

$$I_{0,\,pn} \cong \sigma_n \nu_{th} N_c \exp\left[-\frac{(E_c - E_F)}{kT}\right]$$

where σ_n=capture cross section for electrons, ν_{th}=average thermal velocity of carriers, N_c=carrier density in conduction band, E_c=conduction band and E_F=Fermi level. In this frame, energy differences $E_C - E_F$, determined from planar configuration of n-a-Si:H film, should be equal to E_A of sandwich type p–n junction. Indeed, coinciding value of 0.36 eV was obtained for forward/reverse directions and depicted in Fig. 3c.

On the other side, similar analysis could be carried out for Schottky type diode. Likewise to p–n diode, A is temperature independent in forward bias direction in the same bias voltage interval. Therefore, relevant current expression would be

$$I_{Sch.} = I_{0,\,Sch} \exp(AV)$$

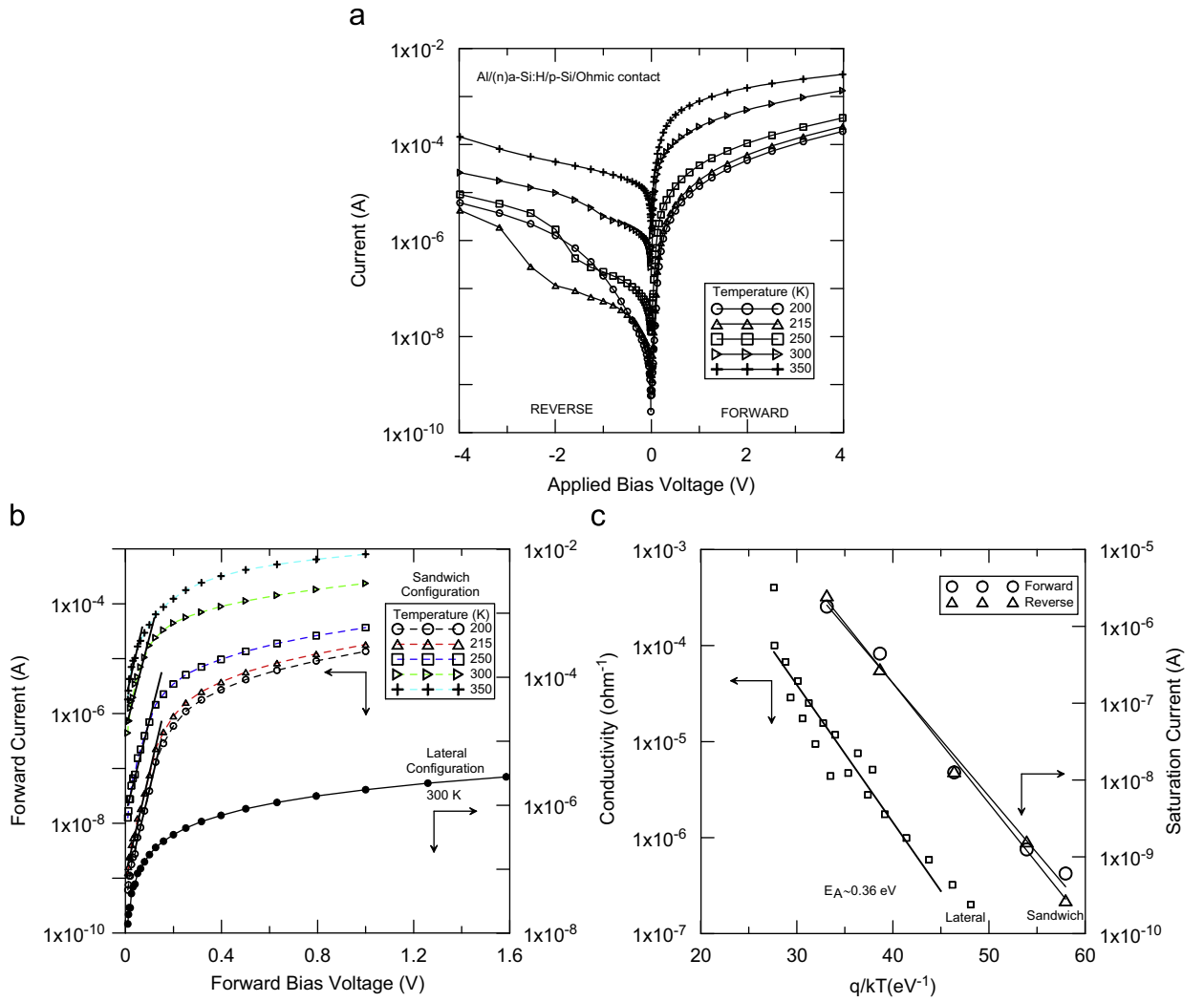

Fig. 3. (a) Forward–reverse I–V characteristic of Al/n-type a-Si:H/p-c-Si/ohmic back contact p–n diode for a wide temperature range (200–350 K). (b) The $\ln I_F$ vs. V_F variation of sandwich type p–n diode (open symbols) for a bias voltage range of 3 kT/q and ~0.2 V. Notice that temperature independent current is obvious, suggesting tunneling mechanism. Full circle, on the other hand, denotes the room temperature I–V characteristic of Al/n-a-Si:H/Al coated glass structure in lateral configuration. (c) Variation of dark conductivity (left side) and saturation current (right side) as a function of reciprocal temperature. Keep in mind that dark conductivity was obtained in lateral configuration whereas saturation current from sandwich type p–n diode yields the same activation energy (E_A) near of 0.36 eV.

Table 2
Slope of $\ln I_F$ vs. V_F as a function of temperature for Schottky and p–n diodes, respectively.

Schottky type		p–n type	
T (K)	A (V^{-1})	T (K)	A (V^{-1})
300	16.4	200	41.9
320	15.8	215	42.9
340	16.0	250	40.0
360	16.0	300	39.1
380	15.5	350	43.5

with

$$I_{0,\,Sch.} \cong \sigma_p \nu_{th} N_v \exp\left[\frac{(E_v - E_F)}{kT}\right]$$

where σ_p, N_v and E_v are capture cross section, density of states and energy level for valance band for holes, respectively.

Slope of $\ln I$ vs. $1/T$ at 0.1 and 0.25 V, shown in Fig. 2c, is equal to 0.18 eV, which is in the proximity of $\phi_B(=(kT/q)\ln(N_v/N_A))$ and denotes E_F–E_v difference. When the forward bias voltage exceeds 0.3 V, different current mechanism dominates the carrier flow for the structures at hand. Log–log plot of I–V indicates a superlinear regime, typical for space charge limited current. Fig. 4a,b illustrates temperature dependence of the exponent of bias voltage for Schottky and p–n diodes, confirming majority carrier injection. Transport features discussed above appear discriminately in C–V characteristic, particularly on the forward bias under low frequency.

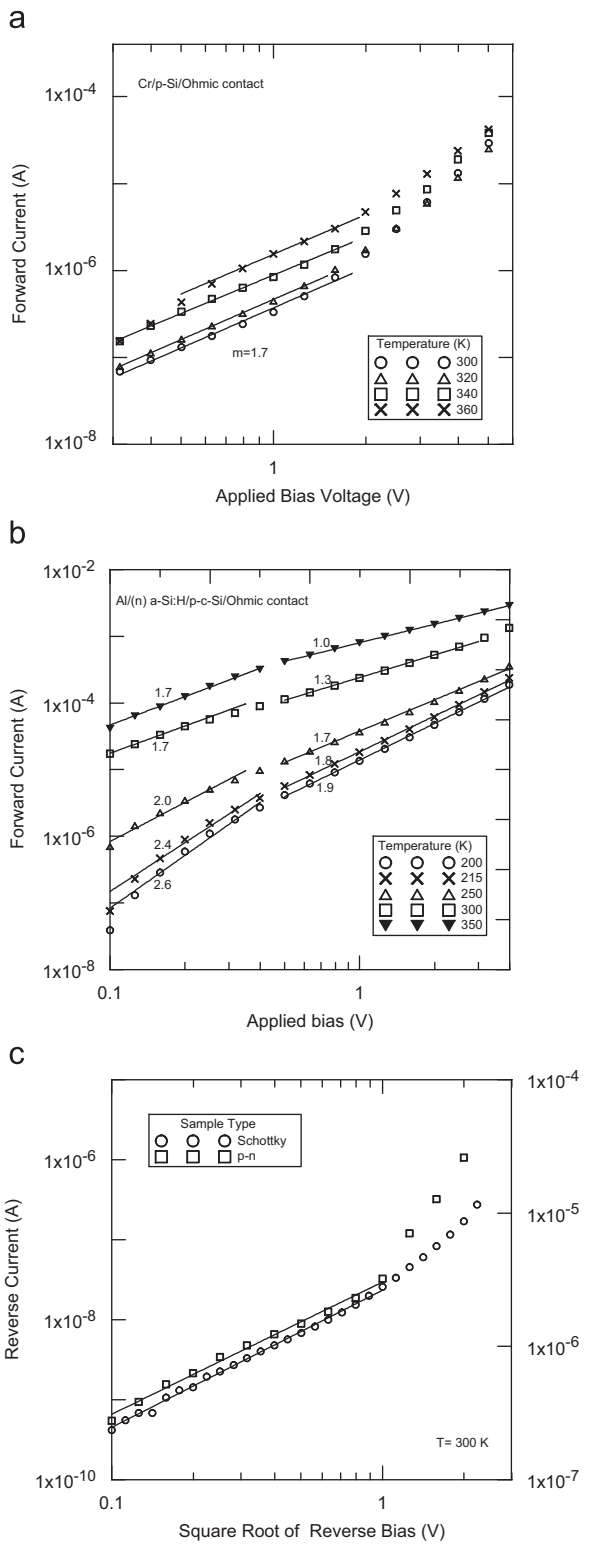

Fig. 4. Power of bias as a function of ambient temperature under forward bias direction for (a) Schottky, (b) p–n diodes. (c) Reverse current vs. square root of reverse bias for Schottky and p–n diodes.

3.2.2. C(G/ω)–V behavior of Schottky and p–n junctions

Figs. 5 and 6 report the normalized capacitances for Schottky and p–n diodes at room temperature under various frequencies as functions of applied bias voltage. Note that the capacitance is normalized to zero bias capacitance value. As clearly seen under forward bias, capacitances of Schottky and p–n junctions increase drastically until maximum point and decrease smoothly afterwards, in other words, a hump emerges. The maxima shifts to the low forward bias and corresponding capacitances become larger as frequency decreases [6]. Remarkably, as ambient temperature is changed from room temperature to higher one (360 K), the shift stop at the specific voltage that corresponds to the built-in voltage ψ_{bi} or barrier height of the metal electrode ϕ_{Bp} [6]. Remarkably, it coincides in value with the one obtained from I to V measurement (0.83 eV). Nevertheless, keep in mind that erroneous ϕ_{Bp} might obtain unless frequency (or temperature) is low (high) enough. In fact, this is another way of determining ϕ_B or ψ_{bi} through C–V measurement [6]. Above ψ_{bi}, due to minority carrier injection (or conductivity modulation), increase in G and parallel decrease in C are eventual. This is comprehensible since C and G are in parallel branch of measured admittance.

For the reverse bias direction, on the other hand, frequency and bias independent admittance value define the depletion layer of the structures at hand. Moreover, square root of reverse current as a function of reverse bias voltage in I–V measurement approve both the existence of such layer (see Fig. 4c) and generation current [5,6,19]. It is assumed here that depletion region exists mostly on a-Si:H side in n-a-Si:H/p-c-Si p–n junction.

The following section is devoted to figure out the hump behavior in C–V in conjunction with the current mechanism in I–V measurement in the light of diagram given in Fig. 7.

4. Discussion

Admittance measurements on Schottky and p–n diodes at hand were performed as a function of dc applied bias voltage, temperature and frequency of bias voltage modulation. At the positive side of voltage, constant voltage independent capacitance corresponded to film geometrical capacitance (C_{geo}). This proposition seemed to agree with those of others [1–4]. The value of 3×10^{-10} F for p–n diode was also verified by inserting appropriate experimentally determined parameters into the relation $C_{geo}=(\varepsilon_{a\text{-}S:H}A/d)$ where $\varepsilon_{a\text{-}S:H}$=permittivity of a-Si:H film ($\approx n^2\approx3.6^2$), $d\sim340$ nm and A=electrode area (9×10^{-3} cm^2). As soon as the bias voltage turned into negative values, majority carriers were involved and caused to drastic rise in capacitance together with strong frequency and temperature dependence in C–V curves. Moreover, the shape of capacitance behavior (demonstrating a peak in capacitance and falling sharply afterward) reminded us diffusion capacitance. Meanwhile, it was observed that current through approximately squarely depends on the applied bias voltage (i.e., V^2) in I–V curve in the same bias

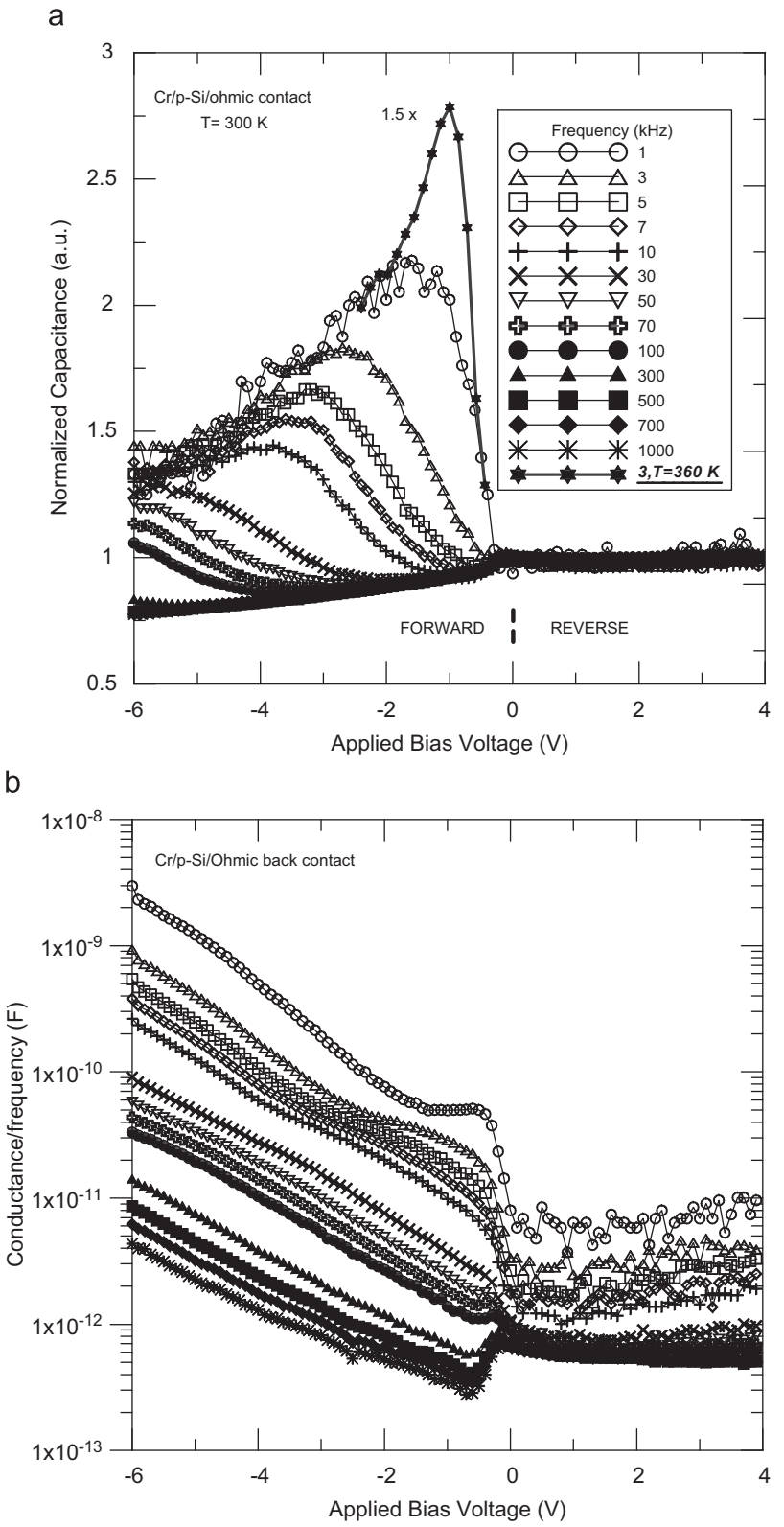

Fig. 5. (a) Normalized capacitance and (b) conductance vs. bias voltage characteristics under various frequencies of Cr/p-c-Si/ohmic contact Schottky diode at room temperature. Also, *C–V* curve measured at 3 kHz under 360 K ambient temperature is depicted.

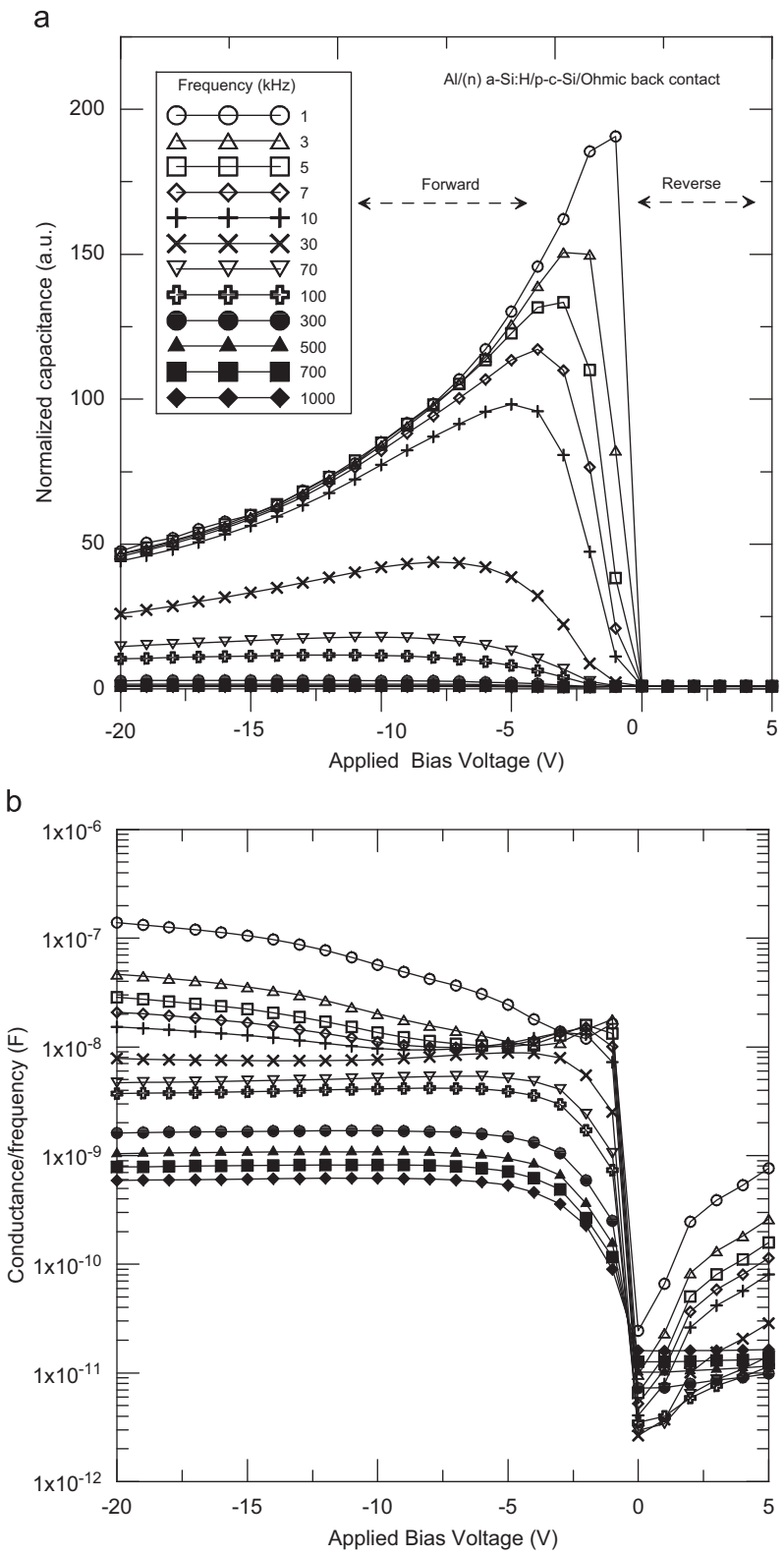

Fig. 6. (a) Normalized capacitance and (b) conductance vs. bias voltage characteristics under various frequencies of Al/n-a-Si:H/p-c-Si/ohmic contact p–n diode at room temperature.

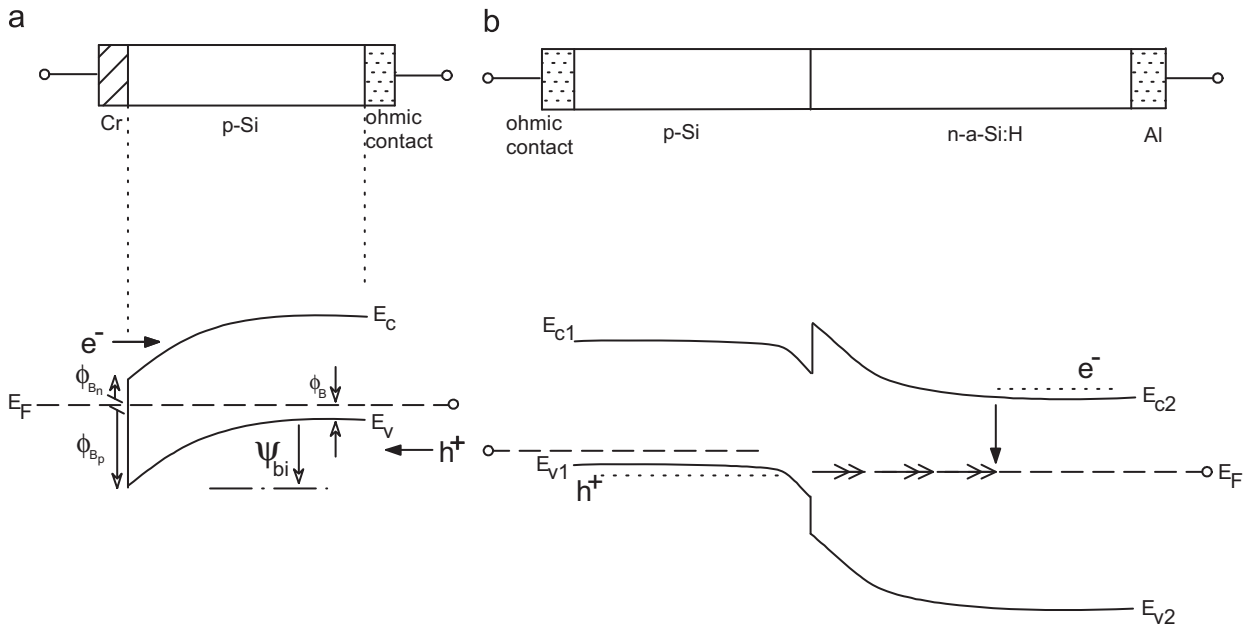

Fig. 7. Schematic current injection processes for (a) Schottky and (b) p–n diodes, inferred through *I–V* and *C–V* measurements.

voltage interval, approving further majority carrier injection [3,4]. Once the bias exceeds the built-in voltage value, decrease in capacitance together with increase in ac conductance was eventual. To be a little more clear, let us expand the argument for a relatively simple case on Schottky diode.

Under forward bias, electrons enter from the metal side whereas holes are injected from the semiconductor side and hence bipolar (ambipolar) transport occurs without non-recombination, causing diffusion capacitance. This scenario seems plausible since barrier height for electrons to surmount would be low compared to that of holes (0.83 eV). Therefore, the remaining barrier (~0.2 eV) corresponds to electrons which would be energy difference of forbidden energy gap of semiconductor and barrier height for majority carriers. If the forward bias gets larger than built-in voltage, some of these minorities jump over the barrier height and/or tunnel through the barrier through interface states between metal and semiconductor and diffuse towards neutral region of semiconductor (see Fig. 7a). In the mean time, equal amount of oppositely charged majorities enter easily from the back ohmic contact to preserve charge neutrality. Consequently, bulk resistance of the diode reduces in other words, conductivity modulation takes place. Correspondingly, this phenomenon manifests as hump like behavior in *C–V* and as increase in *G–V*.

For the p–n diode, on the other hand, MSTCE model we can say the actual carrier flow mechanism in *I–V* measurement and is depicted schematically in Fig. 7b. Briefly, a hole in the valance band of p-c-Si jump from one localized state to another in the depletion region of n-a-Si:H film through tunneling until recombining with electron which is supplied from conduction band of n-a-Si:H film. This multistep tunneling becomes weaker at the edge of depletion layer due to reduced electric fields and most probable recombination takes place there. Actually, this mechanism is one of the models offered for excess current in tunnel diodes by Riben [20]. Descriptive model based on transport feature as to *I–V* measurement on p–n structure can be interpreted in *C–V* measurement: provided the minority carrier concentrations become comparable with the equilibrium concentration ($p \approx N_D$), storage type behavior turns into inductive type which can also be interpreted as negative capacitance. The inductive contribution, in other words, modulation of series resistance due to hole injection, requires time and hence delay between the applied voltage and ac current occurs. Therefore, once *C* becomes inductive, the forward bias voltage reflects the inversion voltage where $p>n$ and hence temperature/frequency dependence is expected and experimentally depicted in Fig. 4a. Eventually, the inductive contribution gets weaker under high frequency or low temperature as illustrated in Figs. 4a and 5a due to the fact that minority carriers cannot follow such high ac voltage modulation.

5. Conclusion

Majority and minority carrier injections took place in the forward direction in a specific bias voltage interval; onset voltage value marked the majority carrier injection where sharp rise in capacitance was eventual whereas decrease in measured capacitance (after passing maxima) denoted the associated voltage where minority carrier injection begins, turning the storage type behavior into inductive, one which is also called negative capacitance.

Acknowledgements

We are grateful to Prof. Dr. Bayram Katırcıoğlu and Assoc. Prof. Dr. İsmail Atılgan for fruitful discussions and production of samples.

References

[1] Garcia-Belmonte Germa, Munar Antoni, Barea Eva M, Bisquert Juan, Ugarte Irati, Pacios Roberto. Charge carrier mobility and lifetime of organic bulk heterojunctions analyzed by impedance spectroscopy. Org Electron 2008;9:847–51.
[2] Bisquert Juan, Garcia-Belmonte Germa, Munar Antoni, Sessolo Michele, Soriano Alejandra, Bolink Henk J. Band unpinning and photovoltaic model for P3HT:PCBM organic bulk heterojunctions under illumination. Chem Phys Lett 2008;465:57–62.
[3] Shrotriya Vishal, Yang Yang. Capacitance–voltage characterization of polymer light emitting diodes. J Appl Phys 2005;97:054504.
[4] Tsai Mei-Na, Chang TC, Liu Po-Tsun, Ko Chung-Wen, Chen Che-jen, Lo Kang-mien. Short diode like diffusion capacitance of organic light emission devices. Thin Solid Films 2006;498:244–8.
[5] Sze SM. Physics of semiconductor devices. John Wiley & Sons; 1969.
[6] Kanicki J. Amorphous and microcrystalline semiconductor devices, materials and device physics, vol. 2. Artech House Inc.; 1992.
[7] Ferreira I, Costa MEV, Pereira L, Fortunato E, Martins R, Ramos AR, et al. Silicon carbide alloys produced by hot wire, hot wire plasma-assisted and plasma-enhanced CVD techniques. Appl Surf Sci 2000;184:8–19.
[8] Catherine Y, Zamouche A, Bullot J, Gauthier M. Ion bombardment effects in plasma deposition of hydrogenated amorphous silicon carbide films: a comparative study of d.c. and r.f. discharges. Thin Solid Films 1983;109:145–58.
[9] Rovira PI, Alvarez F. Chemical (dis)order in a-$Si_{1-x}C_x$:H for $x<0.6$. Phys Rev B 1997;55:4426–34.
[10] Katayama Y, Usami K, Shimada T. Philos Mag B 1981;43:283.
[11] Demichelis F, Pirri CF, Tresso E, Stapinski T. J Appl Phys 1992;71:5641.
[12] McKenzie DR. Infrared absorption and bonding in amorphous hydrogenated silicon–carbon alloys. J Phys D: Appl Phys 1985;18:1935–48.
[13] Swaaij RACMMV, Berntsen AJM, Van Sark WGJHM, Herremans H, Bezemer J, Van der Weg WF. J Appl Phys 1994;76:251.
[14] Bullot J, Schmidt MP. Phys Status Solidi (b) 1987;143:345.
[15] Tawada Y, Tsuge K, Condo M, Okamoto H, Hamakawata Y. J Appl Phys 1982;53:5273.
[16] Weider H, Cardona M, Guarnieri CR. Phys Status Solidi B. 1979;62:99.
[17] Lucovsky G. Chemical effects on the frequencies of Si–H vibrations in amorphous solids. Solid State Commun 1979;29:571–6.
[18] Stachowitz R, Fuhs W, Jahn K. Low temperature transport and recombination in a-Si:H. Philos Mag 1990;B62:5.
[19] Matsuura H, Okuno T, Okushi H, Tanaka K. Electrical properties of n-amorphous/p-crystalline silicon heterojunctions. J Appl Phys 1984;55:1012–9.
[20] Riben AR, Feucht DL. Electrical transport in nGe–pGaAs heterojunctions. Int J Electron 1966;20:583–99.